Hyperfine structure and isotope shift of 3.5-h ^{193}Hg by a Zeeman-scanned optical-pumping method*

G. F. Fulop, C. H. Liu,† P. A. Moskowitz,‡ O. Redi, and H. H. Stroke
Department of Physics, New York University, New York, New York 10003
(Received 12 September 1973)

A new method, suggested by work of Otten, involving Zeeman scanning of an optically pumped vapor has been developed and used to determine the hyperfine structure of 3.5-h ^{193}Hg ($I=\frac{3}{2}$) in the $6s6p\ ^3P_1$ state, and the isotope shift in the 2537-Å resonance line. The $6s^2\ ^1S_0$ ground state is optically pumped via each of the hfs components. The displacements of the ^{193}Hg hfs components from ^{198}Hg are found by measuring the magnetic field used to scan the optical-pumping lamp. The resonance is detected optically. The measured values are 83(4), 572(5), and 911(5) mK for the $F=\frac{5}{2}, \frac{3}{2}$, and $\frac{1}{2}$ components, respectively. The final results are 80(7) and 572(5) mK for the positions of the first two components corrected to account for perturbations caused by the presence of other isotopes. These perturbations are much smaller than the ones encountered in optical spectroscopy because of the selective nature of our detection method. A model calculation for the relevant emission and absorption processes was developed to determine the perturbations. We obtain, with the use of the previously determined A value, the corrected quadrupole interaction constant $B=+15(7)$ mK. The corrected isotope shift of ^{193}Hg relative to ^{198}Hg is 383(7) mK. The resulting corrected odd-even staggering parameter, relative to ^{192}Hg and ^{194}Hg, is $\gamma=0.74(30)$ or 0.56(14), the two values corresponding to different measurements of the isotope shift of ^{192}Hg.

I. INTRODUCTION

As part of a systematic study[1] of nuclear charge and magnetization structures we have measured the hyperfine structure and isotope shift (relative to ^{198}Hg) in the $6s^2\ ^1S_0$-$6s6p\ ^3P_1$ 2537-Å resonance line of 3.5-h ^{193}Hg. The results were expected to extend the understanding of the isotope shifts and, in particular, the odd-even staggering effects which have been observed in the isotopes of mercury.[2]

Since mercury is a heavy element, its isotope shifts are due almost exclusively to the nuclear charge volume and deformation-dependent effects.[3] In the former, the isotope shift reflects the change in nuclear charge radius with neutron number, assuming a spherically symmetric distribution. In the latter, the nuclear volume is assumed to be constant and the shift is attributed to deformations of the nuclear charge distribution.

The nuclear spin I of ^{193}Hg has been determined previously from the $6s7s\ ^3S_1$-$6s6p\ ^3P_0$ 4047-Å transition to be $\frac{3}{2}$.[4] There are therefore three hfs components in the $^3P_1$ state, the upper state of the 2537-Å resonance line. Attempts to observe these components with the techniques of optical spectroscopy were made by us[2,5] and by Davis, Aung, and Kleiman.[6] In our previous work we were able to observe only the total angular momentum $F=\frac{3}{2}$ hfs component, the others being overlapped by the hfs components of other isotopes (^{193m}Hg and ^{196}Hg) produced simultaneously in the cyclotron bombardment. The details of the production of ^{193}Hg by the reaction ^{197}Au $(p, 5n)$ ^{193}Hg have been summarized by us recently.[7] In this work we relied, in addition to the direct production of ^{193}Hg, on the feeding by the decay of the 11-h ^{193}Hg isomer.

Davis, Aung, and Kleiman succeeded in avoiding the spectroscopic overlap problem by using two different methods of isotope production. At high α-particle energies the reaction ^{197}Au $(\alpha, 8n)$ ^{193}Tl $(\beta^+)\rightarrow$ ^{193}Hg produced very little ^{196}Hg so that the ^{193}Hg $F=\frac{5}{2}$ component could be measured. At low α-particle energies, very little ^{193m}Hg was produced in the reaction ^{194}Pt $(\alpha, 5n)$ ^{193m}Hg, thus permitting measurement of the ^{193}Hg $F=\frac{1}{2}$ component. Thus they obtained the magnetic dipole and electric quadrupole interaction constants, $A=-200(10)$ mK and $B=+40(20)$ mK, and a value of the isotope shift (relative to ^{198}Hg) equal to 412(16) mK.

A more accurate A value of $-204.6(5)$ mK was obtained by Redi and Stroke[8] from a measurement of the "principal" level crossing of ^{193}Hg.

An obvious sequel to obtain a more precise result for the quadrupole interaction constant B is to perform a second level-crossing measurement. (We recall that level-crossing results are not affected by Doppler broadening as are optical spectroscopic measurements.) However, the large uncertainty in B, together with the prediction by Sharon,[9] based on a systematic study of signs of quadrupole moments, that for ^{193}Hg the sign should be negative, led to an unreasonably large region of search

in magnetic field (~8000 G) for locating this second level crossing. We note also that for the B value of Davis *et al.* there is no "fold-over" $\Delta m = 2$ crossing, i.e., a crossing of magnetic sublevels arising from the same F level. In addition, the search was rendered difficult by the fact that the signal strengths of the remaining crossings in mercury are considerably weaker than that of the "principal crossing" that we measured earlier.

After several fruitless attempts to observe with our present techniques additional level crossings in ^{193}Hg, including those for which $\Delta m = 1$, we looked for a method that would eliminate the aforementioned effects of overlap by other isotopes in the optical spectrum.

II. NEW ZEEMAN-SCANNED OPTICAL-PUMPING METHOD

One property that is distinct for all of the odd mercury isotopes is the nuclear g factor. It can be measured by means of NMR following optical pumping[10,11] of the diamagnetic ground state. We were thus led to a method first proposed by Otten[12] for the study of short-lived radioisotopes. In his experiments, the Zeeman-shifted light from a stable-isotope lamp is used to produce nuclear orientation through optical pumping; this is detected by the resulting β-decay asymmetry. These experiments were made "on-line" at the project ISOLDE (Isotope Separation with On-Line Detection) at CERN (Centre Européen de la Recherche Nucléaire, Geneva).

In the adaptation of the method to our problem, we first optically pump the ^{193}Hg atoms in the $^1S_0$ ground state. This was accomplished with the use of a single circularly polarized light beam, incident at 45° with respect to the static magnetic field. A rf field, resonant at the energy difference of the magnetic sublevels, was also applied. This produced a coherence among the magnetic sublevels which resulted in the modulation of the light beam. The intensity of this modulated light beam was monitored as a function of the wavelength tuning of the 2537-Å radiation. We described the details of our optical-pumping method, which is a variation of that of Bell and Bloom, in Ref. 7. None of the other isotopes contribute to the NMR-modulated light signal, even though possibly optically pumped, since their nuclear g factors are different from ^{193}Hg.

We contrast our present technique with the earlier absorption method of optical pumping. There, circularly polarized 2537-Å radiation is tuned to excite a particular hfs level in the $^3P_1$ state. The resulting selective excitation of particular magnetic levels, followed by reradiation to the ground state, also produces an unequal population among the ground-state magnetic sublevels. An orientation (different populations of atoms in positive and negative magnetic sublevels) can thus be established with a resulting net magnetization. The equilibrium population can be reestablished by applying a rf field resonant at the energy difference of the magnetic sublevels.

In both experiments the optical pumping is achieved by means of a Zeeman-scanned ^{198}Hg lamp. Its wavelength, or frequency, can be tuned (by means of magnetic field variations) to make the energy difference in a transition between one of the ^{198}Hg $^3P_1$ excited-state and ground-state magnetic sublevels coincide with the zero-field excitation energy of a particular ^{193}Hg $^3P_1$-state hfs component of interest. Therefore, by measuring the strength of a NMR signal as the ^{198}Hg wavelength is tuned through the values required to produce optical pumping via the three excited-state hfs components, we can obtain the 2537-Å spectral line profile of *all three* ^{193}Hg components. (We shall refer to the resulting curves as "scanning profiles.")

This method is similar in principle to the Zeeman-scanning experiments of Sagalyn, Melissinos, and Bitter[13] in which the $^3P_1$-state hfs magnetic sublevels are also excited selectively with the use of polarized light, but where optical double resonance[11] (resonance among *excited*-state sublevels) is combined with magnetic scanning to discriminate between overlapping lines.

It should also be pointed out that our method is quite general and can be applied to the measurement of the hfs and isotope shift of any isotope that can be optically pumped.

III. EXPERIMENT

A. Apparatus

Figure 1 shows the arrangement used in the Zeeman-scanned optical-pumping experiments. With the exception of the exciting lamp and of the scanning magnet, the apparatus is essentially the same as that used in our optical-pumping experiments,[7] where we measured the nuclear magnetic moments of a series of mercury radioactive isotopes. The incident resonance radiation was obtained from an air-cooled electrodeless ^{198}Hg lamp excited at a frequency of 3 GHz with microwave radiation obtained from a QK-61 magnetron (not shown in Fig. 1).

The lamp was located in a magnetic "scanning field" which was used to tune the emitted ^{198}Hg radiation over the hfs levels of interest. The light from the lamp was made to pass through a series of quartz lenses, following which it was circularly

polarized with the use of a linear polarizer (type PL-40, Polacoat, Blue Ash, Ohio), the transmission axis of which was oriented perpendicularly to the scanning field, and a quarter-wave plate (Valpey–Fisher, Holliston, Mass.).

The circularly polarized light pumped the atoms in the resonance cell. The cell was located in a weak magnetic field $H_0(\approx 5$ G) produced by a pair of Helmholtz coils (not shown in Fig. 1). The Helmholtz field was oriented at 45° with respect to the direction of the incident light. In this way a single beam is used for both pumping and monitoring the degree of orientation. We presented details of the optical-pumping signal obtained with the use of this geometry in Appendix I of Ref. 7.

The cell walls were maintained at a temperature of approximately 200°C with the use of a Bunsen burner. This was necessary, in particular, to maintain the small number of atoms in the vapor phase. It also reduced the dwell time of the mercury atoms on the walls, and thereby increased the optical-pumping relaxation time.[7]

An oscillating field H_1 was applied at right angles to H_0. In the case of the $^1S_0$ state of mercury we are observing nuclear magnetic resonance and H_1 is actually an audio-frequency field. When the frequency of H_1 coincides with the NMR frequency ω_L, transitions are induced among the ground-state sublevels in the resonance. As noted earlier, the coherence thus established between the Zeeman sublevels causes the light emitted from the cell to be modulated. After passing through a 2537-Å interference filter, the light was incident on a photomultiplier tube. The large dc background was eliminated with the use of RC coupling. The signal, at frequency ω_L, was then impressed on a preamplifier (model 103, Keithley Corp., Cleveland, Ohio). The resulting signal was detected by a lock-in amplifier (Princeton Applied Research model HR-8), the reference of which was the oscillating frequency. The signals were usually stored in the memory of a signal averager (however, single sweeps were actually found adequate). These were recorded later with the use of an X-Y recorder.

1. Light sources

The lamp consisted of a 1-cm-diam quartz bulb which contained approximately 1 mg of enriched ^{198}Hg and 1–2 Torr of argon carrier gas. The isotopic composition was 94, 3.9, and 1% for ^{198}Hg, ^{199}Hg, and ^{200}Hg, respectively, and less than 1% for all the other isotopes. As mentioned previously, it was excited with the use of a magnetron. The stability of the lamp depended to a great extent on the use of a well-regulated current power supply. Thus an inferior quality power supply, used for the initial tests, was found inadequate for the more important radioactive runs and it was replaced by a Hewlett–Packard model 6225A precision regulated power supply. Furthermore, in all of the measurements of ^{193}Hg the filament current of the magnetron was supplied by a 6-V storage battery so as to minimize ripple. The light scattered from one of the quartz lenses was detected by a RCA 1P28 photomultiplier (designated by "Monitoring P. M." in Fig. 1) and served to monitor the variations of lamp intensity. The measurements were made with a photometer (model 15, Pacific Photometric Instruments, Berkeley, Cal.). It was found that the optical-pumping signal S was approximately proportional to this monitoring output current i_m, which, in turn, was proportional to the light intensity:

$$S = Ki_m, \tag{1}$$

where K is a proportionality constant. For changes Δi_m in the photomultiplier current we have, therefore,

$$\Delta S = K\Delta i_m. \tag{2}$$

The constant K could be determined by measuring ΔS for a small intensity change Δi_m of the lamp

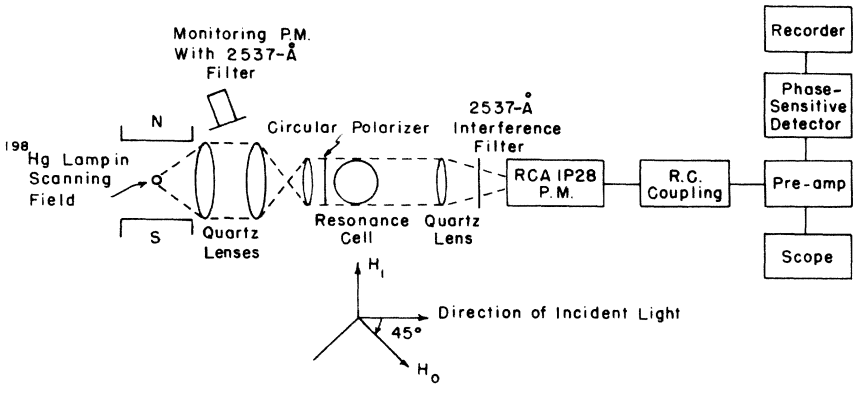

FIG. 1. Schematic of optical-pumping and magnetic scanning apparatus.

(by varying the magnetron current). Once we know the value of K, the effect of all subsequent changes in Δi_m can be obtained from Eq. (2). In general, K was evaluated for each scanning profile.

The changes ΔS caused by light intensity variations never exceeded 10% for the scanning of a complete profile (typically 1000–1500 G). Where necessary, appropriate compensation was made in the optical-pumping signal strength for this small variation. However, for the purpose of locating the line center the scanning of only a region of 300–400 G was needed, provided that the line center is assumed to be at the peak. We show below that this is a reasonable assumption. Over such a region the variations in ΔS were always less than 1% and therefore negligible.

2. *Scanning field*

The lamp was placed between the pole pieces of a 12-in. electromagnet (Varian model V-4012-3B). For the pumping of the natural isotopes, the 12-in. pole pieces were used while in the case of ^{193}Hg, tapered 5.5-in. pole pieces were necessary so as to be able to attain a field of 15 kG.

The scanning field was measured with the use of a rotating-coil gaussmeter having an accuracy of 0.01% (model 924, Rawson–Lush, Acton, Mass.). The gaussmeter was checked periodically against a NMR gaussmeter and it was found to maintain its nominal accuracy. For measurements above 11 111 G (the upper limit of the model 924 gaussmeter) the range of the decade dials was extended with no loss in accuracy.

The gaussmeter probe was located as close as possible to the lamp without touching it. With the use of the 12-in. pole pieces and a 4-in. gap, good field homogeneity was obtained, and the lamp-to-probe correction was always less than 1 G. With the tapered 5.5-in. pole pieces the lamp-to-probe correction could become as large as 20 G when operating in high fields in the vicinity of 15 kG.

B. Procedure and measurements

The procedure used was as follows: First the scanning field was set so as to excite the hfs component of interest. Then the Helmholtz field was swept through the region in which the optical-pumping signal was expected. Generally, it was more convenient to hold the frequency of H_1 fixed and sweep the Helmholtz field, although the procedure could be inverted. Before proceeding any further, at least five of these optical-pumping resonances were recorded to ascertain that there were no fluctuations in their amplitudes. A typical optical-pumping signal is shown in Fig. 2.

Next, the monitoring photomultiplier tube (Fig. 1) was "calibrated," as described in Sec. III A1. In this way one could observe how changes in photometer current affected the amplitude of an optical-pumping signal. Finally, the scanning field was varied and the relative optical-pumping signal strength recorded for each field point. The lamp intensity was also monitored at each field point. In the few instances when we found it necessary, we normalized the relative optical-pumping signal strength for any changes in the lamp intensity that may have resulted from a variation of scanning field. We thus obtained a plot of corrected signal value vs scanning field.

The position of the peak of such a scanning profile is then the position of the hfs component being resonated. These scanning profiles are discussed in detail in the next section.

1. *Measurements of ^{193}Hg*

Two radioactive runs were performed in which the locations of the three ^{193}Hg hfs components in the $6s6p\,^3P_1$ state, having $F=\frac{1}{2}, \frac{3}{2}, \frac{5}{2}$, were determined by Zeeman scanning of the optical-pumping signals. The numbers I and II are used to identify the corresponding results. Typical scanning profiles are shown in Figs. 3–5. The location of the peak of a particular profile represents the separation betweeen the ^{193}Hg hfs component and the ^{198}Hg zero-field level. The results of all the measurements made with ^{193}Hg are shown in Table I.

The center of each profile was measured in two different ways: (i) from the location of the peak and (ii) from the bisector of the half-intensity points (these are labeled by the letter C and an arrow, on the profiles in Figs. 3–5). The intensity of the lamp was constant over all the profiles obtained during run II. The lamp intensity was not monitored during I.

The error bars shown in the scanning profiles reflect the background noise which was observed on either side of an optical-pumping signal. These error bars make it possible to shift the profiles

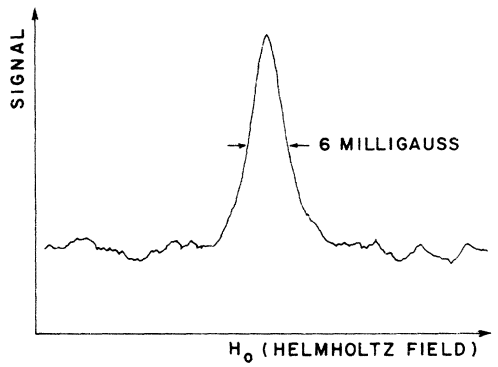

FIG. 2. A NMR signal for optically pumped ^{193}Hg.

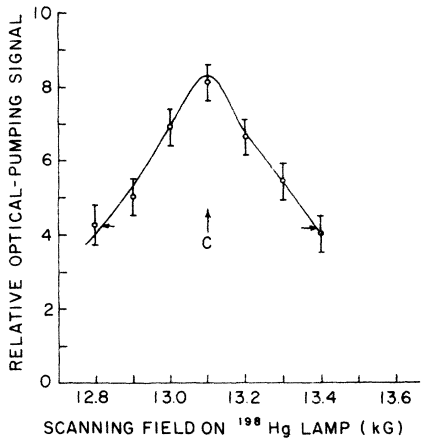

FIG. 3. Zeeman-scanned optical-pumping profile for ^{193}Hg $F=\frac{1}{2}$ component (run II). The cell temperature was 200°C and its tail was at 20°C. C bisects the full width at half-maximum.

slightly from their indicated positions. These shifts are the uncertainties indicated in parentheses in Table I. An analysis of possible systematic errors is given in Sec. III B2 below and in the Appendix.

2. Measurement of natural mercury—analysis of technique

In order to analyze meaningfully the results of the Zeeman-scanned optical-pumping profiles given in Table I, it was necessary to test the procedure by locating the positions of several hfs components that have been measured accurately by other methods. Natural mercury was well suited for these tests.

Natural mercury consists of the isotopes with the mass numbers 204 (7.85), 202(29.80), 201(13.22),

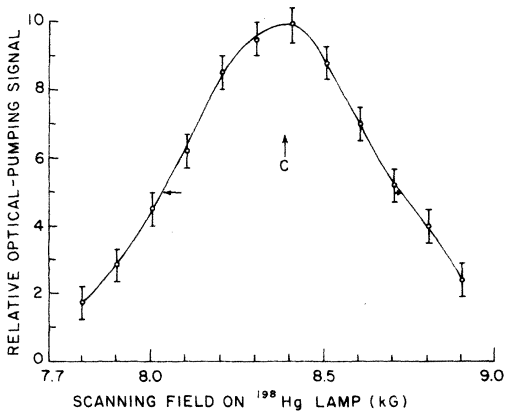

FIG. 4. Zeeman-scanned optical-pumping profile for ^{193}Hg $F=\frac{3}{2}$ component (run II). The cell temperature was 200°C and its tail was at 20°C. C bisects the full width at half-maximum.

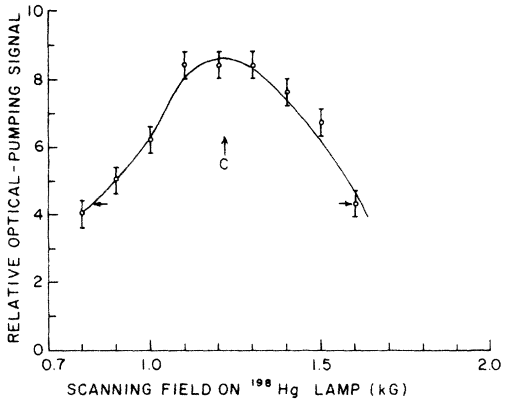

FIG. 5. Zeeman-scanned optical-pumping profile for ^{193}Hg $F=\frac{5}{2}$ component (run II). The cell temperature was 200°C and its tail was at 20°C. C bisects the full width at half-maximum.

200(23.13), 199(16.84), 198(10.02), and 196(0.15), where the percent abundances have been indicated in parentheses. Of these, only the odd-spin isotopes ^{199}Hg ($I=\frac{1}{2}$) and ^{201}Hg ($I=\frac{3}{2}$) can have their $^1S_0$ ground state optically pumped. Thus we have available for a test of the accuracy of the method the natural-mercury hfs components ^{199}Hg $F=\frac{1}{2}$, $\frac{3}{2}$ and ^{201}Hg $F=\frac{5}{2}$, $\frac{3}{2}$, $\frac{1}{2}$. The energy locations of these components have all been measured with accuracies better than 1 mK by Schweitzer.[14]

The Zeeman-scanned optical-pumping profiles of two of these hfs components are shown in Figs. 6 and 7. As before, we measured the center of each profile in two different ways: (i) from the peak and (ii) from the bisector of the half-intensity points. In addition, the line positions measured by Schweitzer are indicated on each of the natural-mercury profiles shown. These values are indicated by an arrow and are labeled "H_{UNPERT}." As in the case of the radioactive measurements, the variations in lamp intensity—as seen by the monitoring photomultiplier tube—were negligible.

Natural-mercury scanning profiles were measured for two different cell geometries, one "peanut" oblong and the other having spherical shape. These yielded identical results within experimental uncertainty.

The results of the measurements of the natural-mercury hfs components are shown in Table II. With the exception of the $F=\frac{3}{2}$ component of ^{199}Hg, where the discrepancies are almost equal, it can be seen that in all cases the difference between the present and Schweitzer's measurements is smaller if the peak line position is used rather than that determined from the half-intensity points. This is especially true for the highly asymmetric profiles of ^{199}Hg ($F=\frac{1}{2}$) and ^{201}Hg ($F=\frac{5}{2}$). The discrepancies are in some cases quite large and outside

TABLE I. Zeeman-scanned optical-pumping measurements of ^{193}Hg. Positions are with respect to the ^{198}Hg zero-field location. The corresponding frequency differences can be obtained with the use of the equivalence 1 G = 2.080 MHz. The hfs components all lie on the high-wave-number side of the ^{198}Hg 2537-Å transition.

		$F=\frac{5}{2}$		$F=\frac{3}{2}$		$F=\frac{1}{2}$	
Run	Scan	Measured from peak (G)	Measured from $\frac{1}{2}$ – intensity points (G)	Measured from peak (G)	Measured from $\frac{1}{2}$ – intensity points (G)	Measured from peak (G)	Measured from $\frac{1}{2}$ – intensity points (G)
I	1	1200 (50)	1260 (50)	8200 (50)	8345 (50)	13 275 (150)	13 320 (150)
	2	1200 (50)	1230 (75)	•••	•••	13 275 (150)	13 397 (150)
II	1	1200 (100)	1265 (50)	8350 (100)	8400 (50)	13 100 (50)	13 100 (50)
	2	1200 (100)	1220 (50)	8350 (100)	8380 (50)	•••	•••
Weighted average of all measurements		1200 (54)	1246 (51)	8250 (58)	8375 (50)	13 131 (55)	13 140 (55)

of the experimental uncertainties shown in parentheses.

A possible reason for these discrepancies is the presence in the cell of other isotopes which have hfs components near the position of the hfs component being magnetically resonated. These perturbing isotopes certainly cannot contribute to the optical-pumping signal of the isotope being resonated—provided that their nuclear g factors are distinct. However, if the perturbing isotope has a hfs component located near (i.e., within one or two Doppler widths) the hfs component of the resonated isotope, it will absorb the incident light and in that way change the effective lamp line shape "seen" by the isotope being investigated.

In Table III we have retabulated the discrepancies shown in Table II in units of mK [we obtain the conversion 1 G = 2.080 MHz with the use of our result[15] $g_J = 1.486110(9)$ and $\mu_B = 1.3996(1)$ MHz/G; we have furthermore 1 mK = 29.9793 MHz] and now refer to the discrepancies as perturbations. We show also the "perturbers," i.e., the hfs components near the ones being resonated. The "perturbing separation" refers to the separation between a resonated line and its perturber, as obtained from Schweitzer's results. The locations of the perturbing isotopes are also indicated in Figs. 6 and 7. It is interesting to note that all of the natural-mercury spectral lines *repel*, as would be expected from preferential absorption.

In order to verify that the perturbations in Table III are indeed due to the presence of other isotopes we performed a Zeeman-scanned optical-pumping experiment on the hfs component ^{199}Hg ($F=\frac{1}{2}$) in a separated-isotope cell, i.e., one containing only ^{199}Hg. As can be seen in Fig. 8, the line center, as measured from the peak, is at the same point as H_{UNPERT} within experimental error. Thus, in a pure-^{199}Hg cell, as expected, we do not see *any* perturbation at all. This is to be compared to the perturbation of 12.7 mK (see Table III) in a natural-mercury cell.

One would also expect that as the temperature of the cell increases two effects would be produced: First, the Doppler widths of both the perturbed and perturbing lines increase; second, in a wet cell, i.e., in which the mercury vapor is in equilibrium with the liquid, the number of absorbing atoms

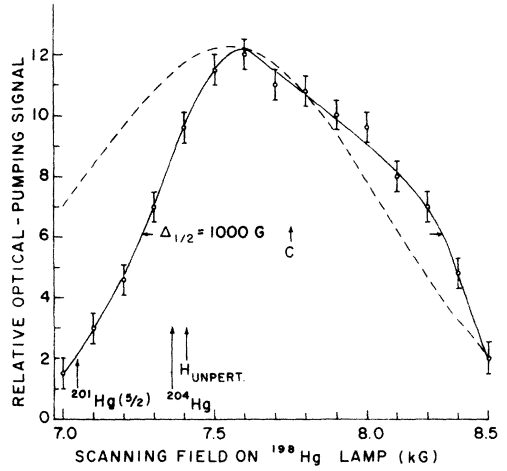

FIG. 6. Zeeman-scanned optical-pumping profile of ^{199}Hg $F=\frac{1}{2}$ component in natural-mercury cell. The excitation was with a ^{198}Hg lamp. The "long-tailed" spherical-shape resonance cell was kept at 200°C and its tail at 20°C. The solid curve is the experimental result. The dashed curve is the calculated prediction, as given in the Appendix, with absorption parameter $k_0 L$ equal to 0.64, 0.75, and 0.78 for ^{199}Hg ($F=\frac{1}{2}$), ^{201}Hg ($F=\frac{5}{2}$), and ^{204}Hg, respectively. C bisects the full width at half-maximum. The locations of the ^{201}Hg and ^{204}Hg perturbing components and of the unperturbed ^{198}Hg component are also shown.

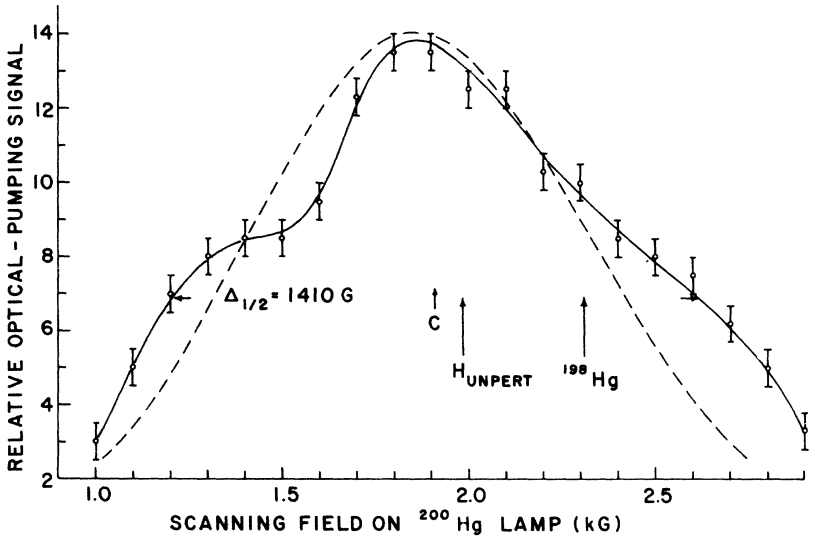

FIG. 7. Zeeman-scanned optical-pumping profile of ^{201}Hg $F=\frac{3}{2}$ component in natural-mercury cell. The excitation was with a ^{200}Hg lamp. The "peanut" oblong shape resonance cell was kept at 200°C and its tail at 20°C. The solid curve is the experimental result. The dashed curve is the calculated prediction, as given in the Appendix, with absorption parameters k_0L equal to 1.14 and 0.50 for ^{198}Hg and ^{201}Hg ($F=\frac{3}{2}$), respectively. C bisects the full width at half-maximum. The locations of the ^{198}Hg perturbing component and of the unperturbed ^{201}Hg component are also shown.

increases. Both of these processes would tend to increase the perturbations. To study this behavior we obtained the scanning profile of the ^{199}Hg ($F=\frac{1}{2}$) hfs component at room temperature (20°C). The perturbation of the peak was found to be 6.2 mK as compared to 12.7 mK at 200°C (see Table III), which is qualitatively what we would expect. The experiments confirm the assumption that it is the presence of the other hfs components which causes the perturbations in the peaks of the scanning profiles.

In the Appendix we discuss a model which allows a quantitative accounting of the perturbations of the spectral lines. A comparison between these calculations and experimental observations is given in Table IV.

3. *^{193}Hg scanning profile corrections and hfs component positions*

We can use the analysis given in the Appendix to determine the location of the hfs components of ^{193}Hg, and, in particular, to estimate the effects of the perturbations by other isotopes present in the resonance cell. The analysis of the natural-mercury scanning profiles showed that better results are obtained when the line center is taken to be the scanning-profile peak rather than the bisector of the half-intensity points. Thus we use only the former values in Table I. With the conversion factors given in Sec. III B 2, these values can be expressed in terms of millikaysers, i.e., 1 mK = 10^{-3} cm^{-1} = 14.413 G. The results for the location of these uncorrected ^{193}Hg hfs components relative to ^{190}Hg are summarized in Table V. The errors given for the $F=\frac{3}{2}$ and $F=\frac{1}{2}$ components have been increased by 1 mK to account for the uncertainty in the magnetic field difference at the positions of the lamp and the measuring probe.

The results are also shown in Fig. 9, in which the perturbing isotopes are also indicated. As discussed in the Appendix, the inclusion of their effects leads to "corrected values" for the location of the scanning peaks. Clearly, the $F=\frac{3}{2}$ component is unperturbed. However ^{193}Hg ($F=\frac{5}{2}$) is perturbed by ^{196}Hg, and ^{193}Hg ($F=\frac{1}{2}$) is perturbed by ^{195m}Hg ($F=\frac{11}{2}$) and ^{193m}Hg ($F=\frac{11}{2}$). From a knowledge of cross sections[16] for the production of ^{196}Hg, and with the use of the Bateman equations for radioactive decay, we estimate that the ratio of ^{193}Hg to ^{196}Hg at the time of the experiment was ≈0.81.

We now assume $(k_0L)_{193(5/2)} \approx (k_0L)_{201(5/2)} \approx 0.75$, where the absorption coefficient k_0 and absorption length L are defined in the Appendix. Both have a nuclear spin $I=\frac{3}{2}$ and therefore any spin-dependent effects are expected to be identical. In Fig. 10 we have plotted the perturbations of ^{193}Hg ($F=\frac{5}{2}$), as calculated from Eq. (A5), vs its unperturbed separation from ^{196}Hg. The perturbation is found to be about 3 mK. Thus we correct the position of the ^{193}Hg ($F=\frac{5}{2}$) component by shifting it 3 mK toward ^{198}Hg. We also add a 3 mK uncertainty which represents an estimate of the accuracy of this correction.

TABLE II. Zeeman-scanned optical-pumping measurements of ^{199}Hg and ^{201}Hg in a natural-mercury cell. The effective Doppler widths of the scanning light and absorbing atoms are, respectively, 900 G (65mK) and 650 G (45 mK). The values are not corrected for perturbations.

hfs component	1 Measured from peak (G)	1 Measured from peak (mK)	2 Measured from $\frac{1}{2}$-intensity points (G)	2 Measured from $\frac{1}{2}$-intensity points (mK)	3 Measured by Schweitzer (Fig. 7) (G)	3 Measured by Schweitzer (Fig. 7) (mK)	4 Discrepancy between 1 and 3 (G)	4 Discrepancy between 1 and 3 (mK)	5 Discrepancy between 2 and 3 (G)	5 Discrepancy between 2 and 3 (mK)
199($\frac{1}{2}$)	7590(75)	526.6(52)	7764(50)	538.7(35)	7407(7)	513.9(4)	183(82)	12.7(56)	357(57)	24.8(39)
199($\frac{3}{2}$)	3210(50)	222.7(35)	3220(100)	223.4(69)	3234(3)	224.4(2)	24(53)	1.7(37)	14(103)	1.0(71)
201($\frac{1}{2}$)	3375(50)	234.2(35)	3390(50)	235.2(35)	3303(7)	229.2(5)	72(57)	5.0(40)	87(57)	6.0(40)
201($\frac{3}{2}$)	450(75)	31.2(52)	480(50)	33.3(35)	325(1)	22.5(1)	125(76)	8.7(53)	155(51)	10.8(36)
201($\frac{5}{2}$)	2050(100)	142.2(69)	1930(50)	133.9(35)	2190(5)	151.9(3)	140(105)	9.8(72)	260(50)	18.0(38)

In the case of the ^{193}Hg ($F=\frac{1}{2}$) component no accurate correction can be made since the locations of the perturbing components are not well known. Consequently, we did not rely on the measurements of this component for our final results.

IV. RESULTS AND DISCUSSION: QUADRUPOLE INTERACTION CONSTANT AND ISOTOPE SHIFT OF ^{193}Hg

In view of the precision of the results that we obtained in these measurements, it is sufficient to evaluate the hfs Hamiltonian[17,18]

$$H = A\vec{I}\cdot\vec{J} + BQ_{op} \tag{3}$$

simply in terms of the magnetic dipole and electric quadrupole interaction constants A and B without corrections for perturbations by other levels.[15] The quadrupole operator in Eq. (3) is given in terms of the nuclear spin $\vec{I}$ and the electronic angular momentum $\vec{J}$ operators as

$$Q_{op} \equiv \frac{3(\vec{I}\cdot\vec{J})^2 + \frac{3}{2}(\vec{I}\cdot\vec{J}) - \vec{I}^2\vec{J}^2}{2I(2I-1)J(2J-1)} . \tag{4}$$

From Eqs. (3) and (4), and the appropriate values $I=\frac{3}{2}$ and $J=1$, we calculate the required matrix elements for the three total angular momentum F levels of ^{193}Hg. The results for the hfs energies E or frequencies E/h (h is Planck's constant), relative to the undisplaced center of gravity (CG) of the level, are

$$\begin{aligned} E/h\ (F=\tfrac{5}{2}) &= \tfrac{3}{2}A + \tfrac{1}{4}B, \\ E/h\ (F=\tfrac{3}{2}) &= -A - B, \\ E/h\ (F=\tfrac{1}{2}) &= -\tfrac{5}{2}A + \tfrac{5}{4}B. \end{aligned} \tag{5}$$

The measured intervals Δ are consequently

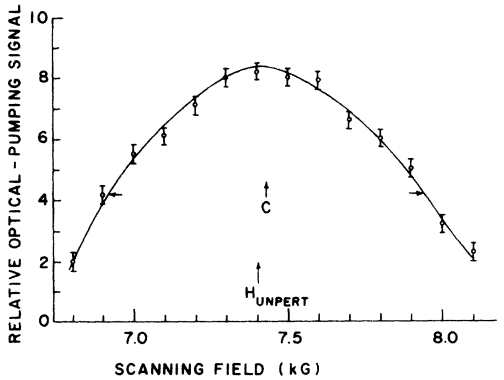

FIG. 8. Zeeman-scanned optical-pumping profile of ^{199}Hg $F=\frac{1}{2}$ component in separated-isotope (86.1% ^{199}Hg) cell. The excitation was with a ^{198}Hg (94% isotopically pure) lamp. The resonance cell was kept at 200°C and its tail at 20°C.

TABLE III. Perturbations of ^{199}Hg and ^{201}Hg hfs components in a natural-mercury cell. All perturbations are positive, i.e., away from the perturbing isotope.

hfs component being perturbed and its isotopic abundance (%)	Perturbation measured from peak (mK)	Perturbation measured from $\frac{1}{2}$ – intensity points (mK)	Perturbing hfs component and its isotopic abundance (%)	Perturbing separations $\Delta\nu$ (mK)
199($\frac{1}{2}$)–16.8	12.7(57)	24.8(40)	201($\frac{5}{2}$)–13.2	25.0
			204–6.8	3.2
199($\frac{3}{2}$)–16.8	1.7(37)	1.0(71)	201($\frac{1}{2}$)–13.2	4.8
201($\frac{1}{2}$)–13.2	5.0(40)	6.0(40)	199($\frac{3}{2}$)–16.8	4.8
201($\frac{3}{2}$)–13.2	8.7(53)	10.7(35)	198–10.0	22.6
201($\frac{5}{2}$)–13.2	9.7(73)	18.0(38)	199($\frac{1}{2}$)–16.8	25.0
			204–6.8	21.8

$$\Delta(F=\tfrac{5}{2}\longleftrightarrow F=\tfrac{3}{2})=\tfrac{5}{2}A+\tfrac{5}{4}B,$$
$$\Delta(F=\tfrac{3}{2}\longleftrightarrow F=\tfrac{1}{2})=\tfrac{3}{2}A-\tfrac{9}{4}B. \quad (6)$$

Note that the $F=\frac{5}{2}$ component lies to the smaller-wave-number side of the center of gravity of the ^{193}Hg 2537-Å transition.

Using our previously measured magnetic dipole interaction constant[8] for ^{193}Hg, we obtain from the $F=\frac{5}{2}\longleftrightarrow F=\frac{3}{2}$ separation the electric quadrupole interaction constant

$$B=18(5)\ \text{mK}\quad\text{(uncorrected)}$$

and

$$B=15(7)\ \text{mK}\quad\text{(corrected for perturbations).}$$

As noted in Sec. III B 3, because of the large uncertainty of the perturbations of the $F=\frac{1}{2}$ component, we do not use it in our final results.

From these hfs components and Eq. (5) we also obtain the isotope shift (Δ_I) relative to ^{198}Hg:

$$\Delta_I(198\text{-}193)=386(4)\ \text{mK}\quad\text{(uncorrected)}$$

and

$$\Delta_I(198\text{-}193)=383(7)\ \text{mK}\quad\text{(corrected).}$$

A quite general observation in isotope-shift measurements has been that relative to even-neutron-number neighbors, the CG of an odd-neutron isotope lies closer to the smaller even-neutron-number partner. We have defined an odd-even staggering parameter to describe this effect as[19]

$$\gamma\equiv\frac{\Delta_I[(N+1)-(N)]}{\frac{1}{2}\Delta_I[(N+2)-(N)]},\quad N\ \text{even}$$

where N is the neutron number. We discuss below the interpretation of γ in the light of nuclear polarizability.

If we use our value[2] for the isotope shifts of ^{194}Hg and ^{192}Hg we obtain

$$\gamma(^{193}\text{Hg})=0.70(27)\quad\text{(uncorrected)}$$

and

$$\gamma(^{193}\text{Hg})=0.74(30)\quad\text{(corrected),}\quad (7)$$

whereas, if we use the values of Davis *et al.*,[6] we obtain

$$\gamma(^{193}\text{Hg})=0.51(11)\quad\text{(uncorrected)}$$

and

$$\gamma(^{193}\text{Hg})=0.56(14)\quad\text{(corrected).}$$

The differences between the corrected and uncorrected values of γ are seen to be negligible when

TABLE IV. Comparison of calculated and observed values of perturbations of natural-mercury hfs components. Note that the parameters for the calculation were obtained by fitting the ^{201}Hg $F=\frac{1}{2}$ component.

Mercury hfs component	Calculated perturbation (mK)	Perturbation from experiment (mK)
199($\frac{1}{2}$)	10.0	12.7(57)
199($\frac{3}{2}$)	1.0	1.7(37)
201($\frac{1}{2}$)	5.0	5.0(40)
201($\frac{3}{2}$)	8.7	8.7(53)
201($\frac{5}{2}$)	11.2	9.7(73)

TABLE V. Positions of ^{193}Hg hfs components relative to ^{198}Hg with corrections for perturbations by neighboring isotopes (see Fig. 9). Uncertainties in the locations of the perturbers relative to the $F=\frac{1}{2}$ component precluded a reliable calculation of its correction.

hfs component F	Uncorrected position (mK)	Corrected position (mK)
$\frac{1}{2}$	911.0(48)	...
$\frac{3}{2}$	572.4(50)	572.4(50)
$\frac{5}{2}$	83.3(37)	80.3(67)

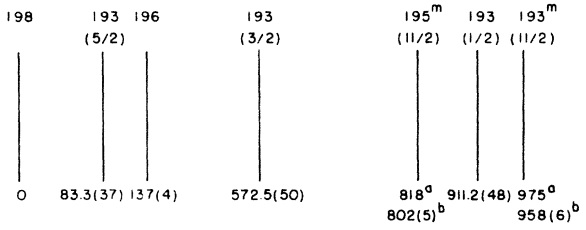

FIG. 9. Hyperfine structure of the 2537-Å line showing the measured positions in mK of the ^{193}Hg components relative to ^{198}Hg and of the possible perturbers. The ^{193}Hg results, corrected for these perturbations, are given in Table V. The measurements of the nuclear isomers are (a) from Ref. 6 and (b) from Ref. 2.

compared to the discrepancy due to different measurements of ^{192}Hg. Thus, in our discussion, we refer only to the corrected values.

In Fig. 11 we plot the staggering parameter as a function of the neutron number for the measured mercury isotopes, including the above results. The central values of $\gamma(^{193}\mathrm{Hg})$ are seen to exhibit appreciable staggering.

We have attempted[2] to interpret odd-even staggering as a measure of the polarization of the nucleus by the outer neutrons. Near the closed neutron shell, $N=126$, the isotope-shift data indicated that added higher-angular-momentum neutrons appear to be more effective in polarizing the nucleus, and hence in producing the changes in the mean value of R^2 of the nuclear charge distribution which are reflected by the isotope shifts.

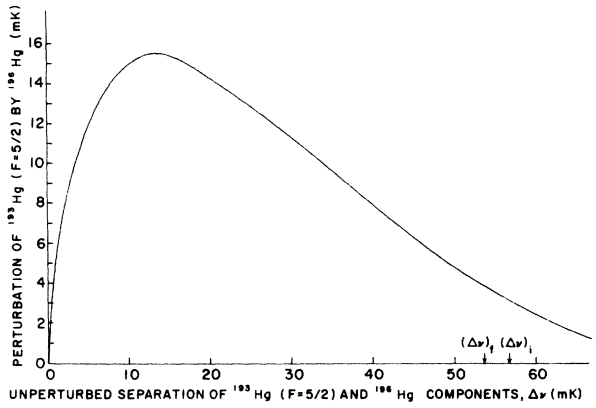

FIG. 10. Calculated perturbation of ^{193}Hg ($F=\frac{5}{2}$) by ^{196}Hg vs the unperturbed separation between the lines. The lamp and cell Doppler-width parameters are α_D =1800 MHz=60 mK, and $\Delta\nu_D$=1300 MHz=43.4 mK. The absorption parameters k_0L are 0.75 and 1.85 for ^{193}Hg ($F=\frac{5}{2}$) and ^{196}Hg, respectively. $(\Delta\nu)_i$ shows the "initial" unperturbed separation (which would be the case if ^{193}Hg were not perturbed) and $(\Delta\nu)_f$ the corresponding "final" perturbed value. The latter is equal to the experimental result.

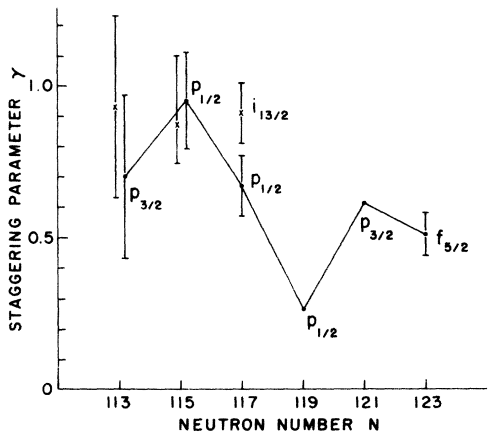

FIG. 11. Plot of the staggering parameter γ as a function of neutron number for the mercury isotopes. The shell-model states of the odd neutrons are indicated. The three points marked with x's refer to the isomeric states with nuclear spin $\frac{13}{2}$. For clarity, the $N=113$ and $N=115$ points are offset slightly along the abscissa. The data for the previous results are given in Ref. 2.

Farther from the closed neutron shell the nucleus should become more readily polarizable and the lower-angular-momentum neutrons become increasingly effective in polarizing the nucleus in this picture.

On this basis, we would expect $\gamma(^{193}\mathrm{Hg})$ to tend toward 1. We would also expect $\gamma(^{193}\mathrm{Hg}) > \gamma(^{201}\mathrm{Hg})$ (see Table VI). We compare these isotopes because both have $I=\frac{3}{2}$. Clearly our results do not give such a high value, although the error brackets in Eq. (7) allow for consistency with the expected trend.

In Table VI we compare nuclear ground-state experimental staggering parameters for mercury with the calculations of Reehal and Sorensen.[20] These are based on the pairing-plus-quadrupole

TABLE VI. Comparison of theoretical and experimental odd-even staggering parameters for mercury.

Isotope	Theory[a]	Experiment[b]
193	0.69	0.70(27)[c]
195	0.88	0.95(16)
197	0.82	0.67(9)
199	0.82	0.270(3)
201	1.00	0.607(3)
203	0.99	0.60(7)[d]

[a] Lowest-order perturbation-theory results of B.S. Reehal and R.A. Sorenson, Nucl. Phys. A 161, 385 (1971).

[b] Values from W.J. Tomlinson, III and H.H. Stroke, Nucl. Phys. 60, 614 (1963), except as noted.

[c] Present work.

[d] O. Redi, Ph.D. thesis (M.I.T., 1965) (unpublished); and O. Redi and H. H. Stroke, Phys. Lett. 8, 257 (1964).

model and consider the isotope shifts to reflect only variations of deformations. The agreement between theory and experiment is seen to be reasonably good for the first three isotopes, though quite poor for the last three. We also note that there are measurements for several nuclear isomers in mercury for which no calculations have been made. Our qualitative interpretation,[19] however, is in reasonable accord for them also.

V. CONCLUSION

A new Zeeman-scanned optical-pumping method has thus been developed for measuring the hfs and isotope shift of any isotope that can be optically pumped. The effects of overlapping lines from other isotopes can be eliminated if their g factors differ from that of the isotope being resonated. However, nonresonating isotopes may still have an effect on the measurements through their influence on the line profile of the exciting light. The result of the isotope-shift measurement shows that ^{193}Hg follows reasonably the trend obtained from the other isotopes. Our measurement of the quadrupole interaction constant should facilitate further level-crossing work which, in turn, will allow a more precise determination of the isotope shift.

ACKNOWLEDGMENTS

We are grateful to Dr. A. Koehler and the staff of the cyclotron at Harvard University for assistance with the bombardments. We also wish to thank Professor W. Happer, Columbia University, and Professor P. Berman, New York University, for stimulating discussions relating to the line-shape problem.

APPENDIX: QUANTITATIVE INTERPRETATION OF PERTURBATIONS IN SCANNING PROFILES—APPLICATION TO NATURAL MERCURY

A complete analysis of the passage of light in an optically pumped medium that would allow a quantitative accounting of the perturbations of the scanning profiles would require a quantum-mechanical calculation along the lines described by Mathur, Tang, and Happer.[21] On the basis of our experimental results with natural-mercury isotopes, the hfs of which are known, we found that a less rigorous and simpler model calculation leads to reasonable agreement with the experimental values.

Let us assume that the lamp emits a spectral line with a Gaussian line shape,

$$I_0(\nu) = C \exp\{-4(\ln 2)[(\nu-\nu')/\alpha_D]^2\},$$

where C is a constant, α_D is the Doppler width of the lamp line, and ν' is the frequency about which the line is centered. A portion of $I_0(\nu)$ will be absorbed by the atoms in the resonance cell and reradiated in all directions. The transmitted intensity, for all frequencies, will then be given by

$$I_T = \int I_0(\nu)\, e^{-k_1(\nu)L}\, d\nu, \tag{A1}$$

where L is the absorption length. The absorption coefficient

$$k_1(\nu) = k_{01} \exp\{-4(\ln 2)[(\nu-\nu_1)/\Delta\nu_D]^2\},$$

centered about the frequency ν_1 with a Doppler width $\Delta\nu_D$, is assumed to be that of the isotope for which we have NMR. The maximum absorption coefficient[22] is given by

$$k_0 = \frac{1}{\Delta\nu_D}\left(\frac{\ln 2}{\pi}\right)^{1/2} \frac{\lambda_0^2}{4\pi} \frac{g_2}{g_1} \frac{N}{\tau}, \tag{A2}$$

where λ_0 is the wavelength of the transition, τ the excited-state lifetime, N the density of the ground-state atoms, and g_2 and g_1 the statistical weights of the excited and ground states, respectively. Suppose that the cell also contains a perturbing isotope which absorbs at the frequency ν_2. (The treatment can be extended simply to any number of perturbing isotopes.) Then Eq. (A1) becomes

$$I_T = \int_{-\infty}^{\infty} I_0(\nu) \exp[-k_1(\nu)L - k_2(\nu)L]\, d\nu$$

or, explicitly,

$$I_T(\nu', \nu_1, \nu_2) = C \int_{-\infty}^{\infty} \exp\{-4(\ln 2)[(\nu-\nu')/\alpha_D]^2 - k_{01} L\, e^{-4(\ln 2)[(\nu-\nu_1)/\Delta\nu_D]^2} - k_{02} L\, e^{-4(\ln 2)[(\nu-\nu_2)/\Delta\nu_D]^2}\}\, d\nu, \tag{A3}$$

where we have assumed that the Doppler widths of isotopes 1 and 2 are approximately the same—a good approximation for the isotopes of mercury. In order to evaluate this integral we make the substitutions $x \equiv (\nu-\nu_1)/\Delta\nu_D$, $\bar{\nu} \equiv \nu_1 - \nu'$, and $\Delta\nu \equiv \nu_2 - \nu_1$. Eq. (A3) then becomes

$$I_T(\bar{\nu}, \Delta\nu) = C\,\Delta\nu_D \int_{-\infty}^{\infty} \exp\{-4(\ln 2)[(x\Delta\nu_D + \bar{\nu})/\alpha_D]^2 - k_{01} L\, e^{-4x^2 \ln 2} - k_{02} L\, e^{-4(\ln 2)[x-\Delta\nu/\Delta\nu_D]^2}\}\, dx, \tag{A4}$$

which is an equation that gives the detected intensity as a function of $\bar{\nu}$, the separation between the lamp and resonated isotope line centers. The first term in the curly brackets of (A4) tends to make $I_T(\bar{\nu}, \Delta\nu)$ peak near $\bar{\nu} = 0$, as expected. However, isotope 2 now also has an influence which depends upon its separation $\Delta\nu$ from ν_1 and on the

relative abundance of isotopes 1 and 2 through the absorption coefficients k_{01} and k_{02}. The selective nature of the optical-pumping process can now be taken into account by noting that only isotope 1 is being resonated. Therefore, all of the time dependence is contained in its absorption coefficient

$$k_{01} = k_{01}(t) = k'_{01} + k''_{01} e^{i\omega_1 t},$$

where k'_{01} is the dc part of the absorption coefficient, k''_{01} is the amplitude of the ac part, and ω_1 is the resonating frequency. Inserting this into Eq. (A4) and Fourier analyzing the time-dependent intensity yields a nonzero Fourier amplitude $I_T(\omega)$ only for ω_1 and its harmonics. Since we are using narrow band detection we will see only the first harmonic, $I_T(\omega_1)$:

$$I_T(\omega_1)(\bar{\nu}, \Delta\nu) = [C k''_{01} L \Delta\nu_D/\omega_1] \times \int_{-\infty}^{\infty} \exp\{-4(\ln 2)[(x\Delta\nu_D + \bar{\nu})/\alpha_D]^2 - k'_{01} L e^{-4x^2 \ln 2} - k_{02} L e^{-4(\ln 2)[x - \Delta\nu/\Delta\nu_D]^2} - 4x^2 \ln 2\}\, dx. \quad \text{(A5)}$$

The last term in the integral tends to peak the signal sharply around $x = 0 (\nu = \nu_1)$ and accounts for the selectivity for isotope 1.

The integral in Eq. (A5) was evaluated numerically on the New York University UNIVAC 1108 computer using a program (Scan 7) developed for this problem. The results are shown by the dashed curves of Figs. 6 and 7.

The effective Doppler width α_D of the lamp has been chosen so as to make the widths of the calculated scanning profiles correspond approximately to those of the experimental profiles. This value, $\alpha_D = 1800$ MHz, has been used throughout these calculations. It can be shown[23] that the calculated perturbations are not very sensitive to the exact value of α_D. For the Doppler widths of the isotopes in the cell we use $\Delta\nu_D = 1300$ MHz, which corresponds to the experimental cell temperature of 200°C.

With the use of Eq. (A2) one can calculate the absorption coefficient k_0 from a knowledge of the lifetime of the $^3P_1$ state and the atom density in the cell. This yields $k_0 = 1.57 \times 10^{-13}(g_2/g_1)N$. If the density N is controlled by a tail temperature of 20 °C then we obtain from the corresponding mercury vapor pressure $N = 4.0 \times 10^{13}$ atoms/cm^3. If we now perform our scanning experiment on ^{201}Hg($F = \frac{1}{2}$), only 13.2% of these atoms will contribute to the absorption coefficient. Thus $(k_0)_{201(1/2)} = 0.415$. Experimentally we measure $(k_0 L)_{201(1/2)} = 0.25$ (see Fig. 12). Thus the effective absorption length for ^{201}Hg($F = \frac{1}{2}$) is $(L_{\text{eff}})_{201(1/2)} = 0.6$ cm, a value quite reasonable for the size of the cells used (diam ≥ 1.5 cm). However, rather than proceed in this manner for all the isotopes investigated, it is more convenient to treat the product $k_0 L$ as a single parameter which one obtains by comparison of theory and experiment. Once we have arrived at a value of $k_0 L$ for a single scanning profile we can use it to predict all subsequent profiles.

The values of $k_0 L$ used in Figs. 6 and 7 were arrived at as follows. The adjustment of $k_0 L$ is most easily done for one of the hfs components ^{199}Hg($F = \frac{3}{2}$), ^{201}Hg($F = \frac{1}{2}$), or ^{201}Hg($F = \frac{3}{2}$), since each one is perturbed by a single perturbing component. For example, for the ^{201}Hg($F = \frac{1}{2}$) component we can plot the perturbations of this component vs $k_{01} L$. This is shown in Fig. 12. A comparison of experiment with the calculations then yields $(k_0 L)_{201(1/2)} = 0.25$.

The hfs components in the $^3P_1$ state of a particular isotope of mercury are well resolved spectroscopically. Thus we never excite more than one of the ^{201}Hg components at a time and, from the

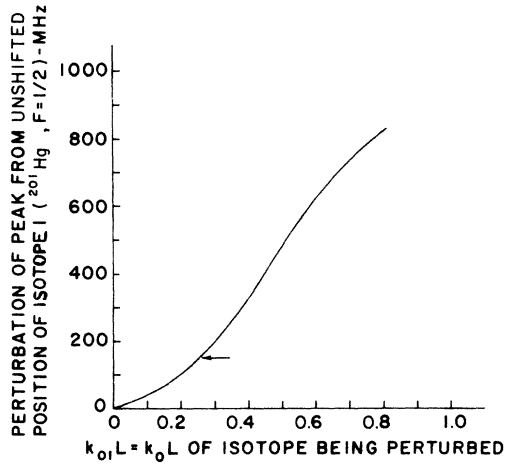

FIG. 12. Calculated perturbation of the ^{201}Hg $F = \frac{1}{2}$ component by the ^{199}Hg $F = \frac{3}{2}$ component vs $k_0 L$ of the perturbed ^{201}Hg. The lamp and cell Doppler-width parameters are $\alpha_D = 1800$ MHz = 60.0 mK and $\Delta\nu_D = 1300$ MHz = 43.4 mK, respectively. The arrow indicates the experimentally observed perturbation obtained by comparing the peak of the corresponding Zeeman-scanned optical-pumping signal with the actual position, as measured by Schweitzer (Ref. 14).

value $(k_0L)_{201(1/2)} = 0.25$, we obtain the corresponding values $(k_0L)_{201(3/2)} = 0.50$, and $(k_0L)_{201(5/2)} = 0.75$ for the remaining ^{201}Hg hfs components with the use of appropriate statistical weights in (A2). With the use of the relative abundances of the natural-mercury isotopes we obtain furthermore $(k_0L)_{199(1/2)} = 0.64$, $(k_0L)_{199(3/2)} = 1.27$, $(k_0L)_{198} = 1.14$, and $(k_0L)_{204} = 0.78$. These values are used in the evaluation of Eq. (A4). The calculations yield the perturbations shown in Table IV.

It can be seen that with the aid of Eq. (A5) we can now predict the perturbations of the natural-mercury absorption line peaks to within about 3 mK. Of course the *actual* line positions are uncertain by the amounts shown in parentheses in Table IV. In addition it can be seen from Figs. 6 and 7 that, although the peaks of the calculated and experimental curves agree reasonably satisfactorily, the asymmetric shape and structure of some of the experimental curves is not well predicted. One of the reasons for this is probably due to the fact that the line shape emitted by the lamp is not a simple Gaussian as we have assumed. If the lamp is not cooled sufficiently it will emit a slightly self-reversed line which will be reflected in the shape of the scanning profile.

In addition our model does not take into account the actual geometry of the experiment, in which different portions of the incident light beam are absorbed by varying thicknesses of mercury vapor.

Lamp impurities, i.e., the presence in the lamp of small amounts of mercury isotopes other than ^{198}Hg, could be expected to contribute to some of the structure in the scanning profiles. However, we found that when we tried to account for this through an additional term in Eq. (A5) weighted according to the relative concentrations of the impurity and of ^{198}Hg, this contribution does not produce the observed structure in the scanning profile.

Finally, we note that illumination with off-resonant light can shift the NMR frequency ("light shift"[11,24]): The shifts are in opposite directions for σ_+ and σ_- light. We verified that in our experiment these shifts produced negligible effects, as can be seen, for example, from the result shown in Fig. 8.

---

*Work supported by the National Science Foundation under Grants GP 15258 and 16676, and in part by the James Arthur Endowment Fund of New York University, and an equipment grant DA-ARO-D-31-124-G763 from the Army Research Office.

†Present address: Department of Physics, University of Arizona, Tucson, Arizona 85721.

‡Present address: Laboratoire de Spectrometrie Physique, Université Scientifique et Médicale de Grenoble, 38041 Grenoble-Cédex, France.

[1]H. H. Stroke, in *Atomic Physics*, edited by B. Bederson, V. W. Cohen, and F. M. J. Pichanick (Plenum, New York, 1969), p. 523; J. Phys. Soc. Jap. Suppl. 34, 543 (1973).

[2]W. J. Tomlinson, III and H. H. Stroke, Nucl. Phys. 60, 614 (1964).

[3]L. Wilets, *Isotope Shifts*, Vol. 38/1 of *Handbuch der Physik* (Springer-Verlag, Berlin, 1958), p. 96.

[4]H. Kleiman, S. P. Davis, and T. Aung, Phys. Lett. 13, 212 (1964).

[5]W. J. Tomlinson, III, Ph.D. thesis (MIT, 1963) (unpublished).

[6]S. P. Davis, T. Aung, and H. Kleiman, Phys. Rev. 147, 861 (1966).

[7]P. A. Moskowitz, C. H. Liu, G. Fulop, and H. H. Stroke, Phys. Rev. C 4, 620 (1971).

[8]O. Redi and H. H. Stroke, Bull. Am. Phys. Soc. 10, 456 (1965); Phys. Rev. (to be published).

[9]Y. Y. Sharon, Nucl. Phys. A 99, 321 (1967).

[10]A. Kastler, J. Phys. Radium 11, 255 (1950).

[11]For a review of the optical and magnetic resonance techniques see *Francis Bitter Selected Papers and Commentaries*, edited by T. Erber and C. M. Fowler (MIT Press, Cambridge, Mass., 1969), Sec. V; and W. Happer, Rev. Mod. Phys. 44, 169 (1972).

[12]E.-W. Otten, Proposal to the Physics III Committee and to the Isolde Committee, CERN, Geneva, 1968 (unpublished); for subsequent work and further references, see J. Bonn, G. Huber, H.-J. Kluge, U. Köpf, L. Kugler, E.-W. Otten, and J. Rodriguez, in *Atomic Physics 3*, edited by S. J. Smith and G. K. Walters (Plenum, New York, 1973), p. 471; and in J. Phys. Soc. Jap. Suppl. 34, 317 (1973).

[13]P. L. Sagalyn, A. Melissinos, and F. Bitter, Phys. Rev. 109, 375 (1958).

[14]W. G. Schweitzer, Jr., J. Opt. Soc. Am. 51, 692 (1961).

[15]O. Redi and H. H. Stroke, Phys. Rev. A 2, 1135 (1970).

[16]N. Poffé, G. Albouy, M. Gusakow, and J. L. Sarrouy, J. Phys. Radium 22, 639 (1961).

[17]N. F. Ramsey, *Molecular Beams* (Oxford U. P., Oxford, England, 1956), p. 272.

[18]C. Schwartz, Phys. Rev. 97, 380 (1955).

[19]W. J. Tomlinson, III and H. H. Stroke, Phys. Rev. Lett. 8, 436 (1962), and additional references therein.

[20]B. S. Reehal and R. A. Sorensen, Nucl. Phys. A 161, 385 (1971).

[21]B. S. Mathur, H. Y. Tang, and W. Happer, Phys. Rev. A 2, 648 (1970).

[22]A. C. G. Mitchell and M. W. Zemansky, *Resonance Radiation and Excited Atoms* (Cambridge U. P., Cambridge, England, 1934), p. 99.

[23]G. Fulop, Ph.D. thesis (New York University, 1971) (unpublished).

[24]C. Cohen-Tannoudji, Ann. Phys. (Paris) 7, 423 (1962); 7, 469 (1962).